ChemComm

Accepted Manuscript

This article can be cited before page numbers have been issued, to do this please use: S. Wu, S. Y. Tan, C. Y. Ang, Z. Luo and Y. Zhao, *Chem. Commun.*, 2016, DOI: 10.1039/C5CC09447J.

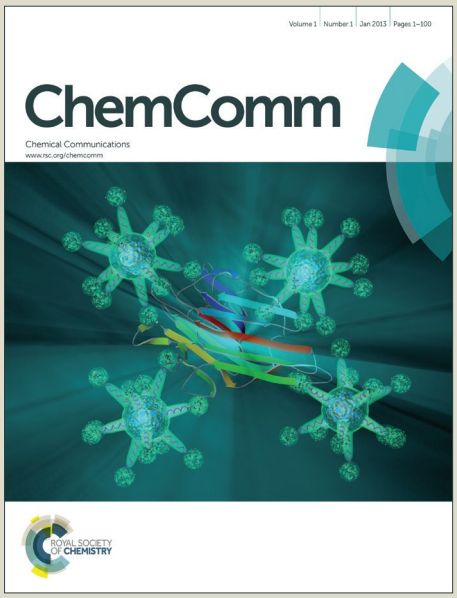

This is an *Accepted Manuscript*, which has been through the Royal Society of Chemistry peer review process and has been accepted for publication.

Accepted Manuscripts are published online shortly after acceptance, before technical editing, formatting and proof reading. Using this free service, authors can make their results available to the community, in citable form, before we publish the edited article. We will replace this *Accepted Manuscript* with the edited and formatted *Advance Article* as soon as it is available.

You can find more information about *Accepted Manuscripts* in the Information for Authors.

Please note that technical editing may introduce minor changes to the text and/or graphics, which may alter content. The journal's standard Terms & Conditions and the Ethical guidelines still apply. In no event shall the Royal Society of Chemistry be held responsible for any errors or omissions in this *Accepted Manuscript* or any consequences arising from the use of any information it contains.

ROYAL SOCIETY OF CHEMISTRY

www.rsc.org/chemcomm

Journal Name

View Article Online
DOI: 10.1039/C5CC09447J

COMMUNICATION

www.rsc.org/

Received 00th January 20xx,
Accepted 00th January 20xx

DOI: 10.1039/x0xx00000x

Oxidation-Triggered Aggregation of Gold Nanoparticles for Naked-Eye Detection of Hydrogen Peroxide

Shaojue Wu,[a,‡] Si Yu Tan[a,‡], Chung Yen Ang[a], Zhong Luo,[a] Yanli Zhao*[a,b]

Naked-eye detecion of H_2O_2 was realized based on the color change of gold nanoparticles upon aggregation. The removal of polyethylene glycol chains from the nanoparticle surface under H_2O_2 treatment let to the exposure of inner hydrophobic ligands, causing the nanoparticle aggregation in aqueous medium. This detection system shows a wide dynamic range in the μM scale and a distinguishable limit of 10 μM.

Hydrogen peroxide (H_2O_2) is an important biologically relevant small molecule. It is the substrate or product of some intracellular enzyme[1,2] and antibody[3,4] involved reactions. In the past years, scientists have studied its complex roles in the mechanisms of some diseases[5-7]. H_2O_2 can also serve as the intermediate object in the detection of disease-related proteins by relying on analytical techniques such as enzyme-linked immunosorbent assay (ELISA)[8-10]. In the ELISA technique, H_2O_2-generating/consuming enzymes like glucose oxidase (GOx) and horseradish peroxidase (HRP) are frequently selected as the label enzymes[9, 10]. The enzyme-induced H_2O_2 concentration change could be measured by colorimetric observation[9-12], plasmonic absorption spectroscopy,[13] or electrochemical detection[14-16]. In particular, the colorimetric method is instrument-free, and in some cases, can provide ultralow sensitivity, which rivals the standard but costly methods[9].

In recent years, gold nanoparticles (AuNPs) have been frequently employed for applications in immunoassays[17-21], based on the property that the frequency of their plasmonic absorption bands shifts with the alteration of their compositions, shapes and aggregation states. Particularly, the color change from red to blue or from blue to red upon aggregation or redispersion of AuNPs can be used as the signal to determine the presence or absence of target proteins in the ELISA technique. Normally, the aggregation of AuNPs could be induced in the presence of di-thiols[22], positively charged thiols,[23] or positively charged biopolymers[24] that are produced from enzyme catalyzed reactions. In addition, the aggregation of AuNPs can also occur during the NP growth in a specific solution involving H_2O_2 as a reducing agent[9], without the presence of cross-linking agents. Since H_2O_2-related enzymes like GOx and HRP are among the most suitable enzymes employed in ELISA[25], developing H_2O_2-responsive signal generation systems would be practically useful in the field of protein detection. In this work, we engineered the surface of AuNPs to be H_2O_2-responsive by incorporating a phenylboronate structure in the surface-adsorbing ligand, so that the surface property of AuNPs can be changed from hydrophilic to hydrophobic upon H_2O_2 treatment, and the accompanied color change in subsequent aggregation state can be harnessed for naked-eye detection of H_2O_2 (Scheme 1).

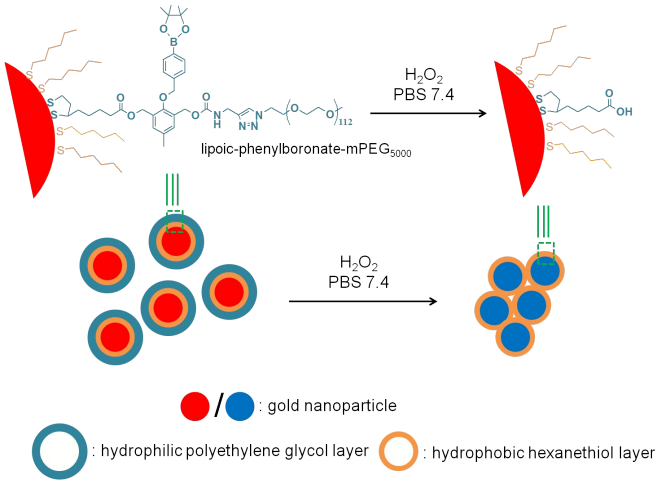

Scheme 1 Schematic representation of H_2O_2 triggered hydrophilicity change and aggregation of AuNPs.

As illustrated in Scheme 1, AuNPs were modified with two ligands: 1-hexanethiol and lipoic-phenylboronate-mPEG$_{5000}$. 1-Hexanethiol is a hydrophobic ligand with a short length, and it forms a hydrophobic layer (indicated as yellow layer in Scheme 1) around AuNPs. Lipoic-phenylboronate-mPEG$_{5000}$ is the ligand with a long hydrophilic polyethylene glycol tail (indicated as cyan layer in Scheme 1). Though the lipoyl and phenylboronate units are hydrophobic, the long polyethylene glycol chain provides excellent

[a]*Division of Chemistry and Biological Chemistry, School of Physical and Mathematical Sciences, Nanyang Technological University, 21 Nanyang Link, Singapore 637371. E-mail: zhaoyanli@ntu.edu.sg; Tel: +65 6316 8792*
[b]*School of Materials Science and Engineering, Nanyang Technological University, 50 Nanyang Avenue, Singapore 639798.*
‡*These authors contributed equally to this work.*
†Electronic Supplementary Information (ESI) available: Additional synthesis and characterization details. See DOI: 10.1039/x0xx00000x

water solubility and steric hindrance to protect AuNPs from aggregation in aqueous medium. The middle phenylboronate entity serves as the H_2O_2-responsive structure, since the phenylboronic ester reacts with H_2O_2 to generate phenyl oxide that initiates quinone methide rearrangement around the aromatic structure and causes the fragmentation of the cresol structure[26-30]. As a result, the polyethylene glycol chain could split from the lipoyl unit and leave the surface of AuNPs. The detachment of the polyethylene glycol chains from AuNPs gradually decreases the water stability and eventually leads to the aggregation of AuNPs along with a red-to-blue color change of the solution. Since the rate of color change depends on the concentration of H_2O_2, different concentrations of H_2O_2 can be discriminated by naked eye.

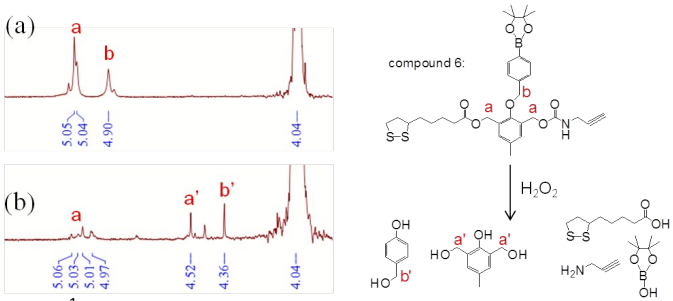

Fig. 1 ^{1}H NMR spectra of compound **6** (a) before and (b) after reaction with H_2O_2 at 37 °C for 70 h. (a) Compound **6** (9.76 mM) in DMSO-d_6 (456 µL) and deuterated PBS (pH 7.4, 130 µL). (b) Compound **6** (9.76 mM) in DMSO-d_6 (456 µL) and deuterated PBS (pH 7.4, 124 µL) containing H_2O_2 (10 M in H_2O, 6 µL, H_2O_2 concentration 96.8 mM). Compound **6** : H_2O_2 = 1 : 10.

The fact that the as-synthesized lipoic-phenylboronate-mPEG$_{5000}$ ligand could undergo the fragmentation in the presence of H_2O_2 was substantiated by ^{1}H NMR characterizations. To simplify the spectrum, compound **6** (Fig. 1), a synthetic precursor of the final lipoic-phenylboronate-mPEG$_{5000}$ ligand, was employed to react with H_2O_2. As shown in Fig. 1a, there are initially no peaks from 4.10 to 4.80 ppm that is the range of ^{1}H NMR peaks for methylene protons of benzyl alcohols. After reacting with H_2O_2 at 37 °C for 70 h, the appearance of two singlet peaks at 4.52 ppm and 4.36 ppm (Fig. 1b) was observed. These two peaks belong to methylene protons of two benzyl alcohols generated from the fragmentation of the middle phenylboronate and cresol units of compound **6**. Correspondently, the intensity of another two peaks at 4.90 ppm and 5.04 ppm belonging respectively to methylene protons of the benzyl ether and benzyl ester of compound **6** disappeared almost completely after the reaction. These changes of ^{1}H NMR spectra prove the hydrolysis of the benzyl ester bonds and the fragmentation of the ligand in the presence of H_2O_2. It is noteworthy to mention that the oxidation of phenylboronate by H_2O_2 could complete within 30 min (Fig. S1a in the ESI), and the hydrolysis of benzyl ether and benzyl ester began and progressed slowly in the next 24 h (Fig. S1b-d in the ESI).

After being used to modify AuNPs, the lipoic-phenylboronate-mPEG$_{5000}$ ligand provides AuNPs with an excellent stability in phosphate buffered saline (PBS, pH 7.4). Since the ligand could not occupy all the surface sites of AuNPs, there are still substantial citrate ligands remained on the AuNP surface. In order to remove these citrate ligands and provide hydrophobicity, an excess amount of 1-hexanethiol was added to the AuNP solution. Without this step of hydrophobization, AuNPs did not aggregate when incubated with H_2O_2. Since the lipoic-phenylboronate-mPEG$_{5000}$ ligand has much stronger binding affinity toward AuNPs, it cannot be replaced significantly by 1-hexanethiol. Thus, the two ligand-modified AuNPs still possess enough solubility and stability in aqueous medium (Fig. 2a). The aggregation of modified AuNPs started at the time of around 4 h with higher concentrations of H_2O_2 (Fig. 2b). For those samples with lower concentrations of H_2O_2, the AuNP aggregation and the color change of the AuNP solutions started after longer hours. At the time of 24 h of incubation, the color change of the AuNP solution with 10 µM H_2O_2 could be clearly discriminated (Fig. 2e and its enlargement). In addition, the transmission electron microscopy (TEM) images of the AuNP solutions before (Fig. 2g) and after (Fig. 2h) the addition of H_2O_2 were recorded. The TEM image shows a significant aggregation of the AuNPs after the treatment of H_2O_2. The intrinsic stability of AuNPs without the addition of H_2O_2 was sufficiently high at the temperature of 37 °C. Only after 43 h of incubation, the AuNP sample started to show some aggregation, and the sedimentation of AuNPs took even longer time (Fig S2i,j in the ESI). The high intrinsic stability of the as-prepared AuNPs elevates the credibility of the experimental test.

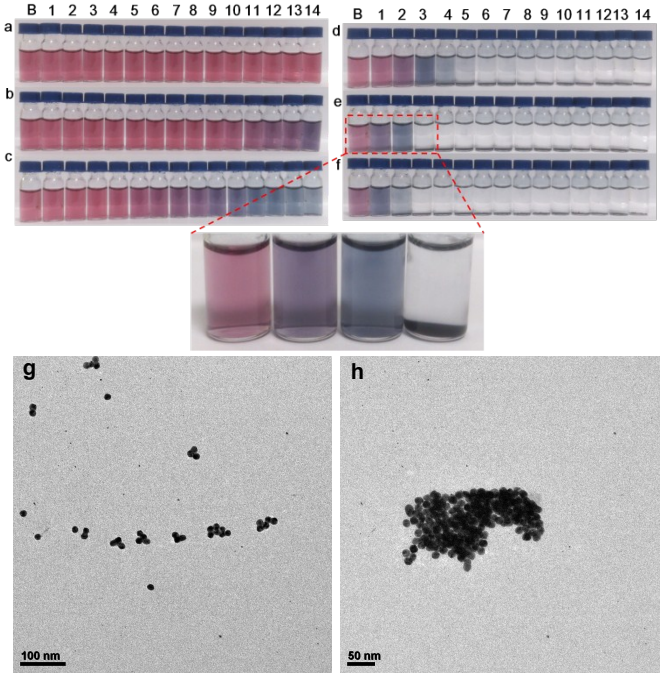

Fig. 2 Gradual aggregation and color change of AuNP solutions incubated with different concentrations of H_2O_2 at 37 °C. Column B: AuNP solution without H_2O_2. Columns 1-14: 10 µM, 20 µM, 40 µM, 70 µM, 100 µM, 120 µM, 160 µM, 200 µM, 300 µM, 400 µM, 600 µM, 800 µM, 1 mM, and 2 mM of H_2O_2. Duration of incubation: a, 0 h; b, 3 h 45 min; c, 6 h 31 min; d, 16 h 24 min; e, 24 h; f, 28 h. TEM images of AuNP solution (g) before and (h) after the treatment of H_2O_2.

The progressing rate of AuNP aggregation in the samples with high H_2O_2 concentration to low H_2O_2 concentration featured linear characteristics. Upon the aggregation, the absorption intensity of AuNPs exhibited a decrease at 527 nm and an increase at 650 nm (Fig. S3 in the ESI). Thus, the ratio of absorption intensity at 650 nm and 527 nm was employed to evaluate the extent of AuNP

View Article Online
DOI: 10.1039/C5CC09147J

aggregation. At the time of 3 h 45 min, only samples with H_2O_2 concentration above 400 μM showed observable color change (Fig. 2b). Fitting of the ratio data matched well with a straight line having a R^2 of 95% (Fig. 3a). At the time of 6 h 31 min, only samples with H_2O_2 concentration above 100 μM showed observable color change (Fig. 2c). The data line of all these samples adopted an "S" shape (Fig. 3b) having a linear middle segment from 100 μM to 600 μM (R^2 99%, Fig. 3c). Finally, the sample with 10 μM of H_2O_2 showed observable aggregation after 16 h 24 min (Fig. 2d). At this time, the samples with H_2O_2 concentration above 40 μM precipitated completely. Only four data could be recorded and fitted to give a curve (Fig. 3d). Since the initial number of the ratio was 0.24 when no aggregation occurred, 0.43 was selected as the threshold for high-confidence discrimination of the color change (Fig. 3e). In summary, the rate of AuNP aggregation under a wide range of H_2O_2 concentrations follows a simple linear rule (or unitary quadratic equation at the lowest concentration zone). This feature may provide an access to quantitative detection of H_2O_2.

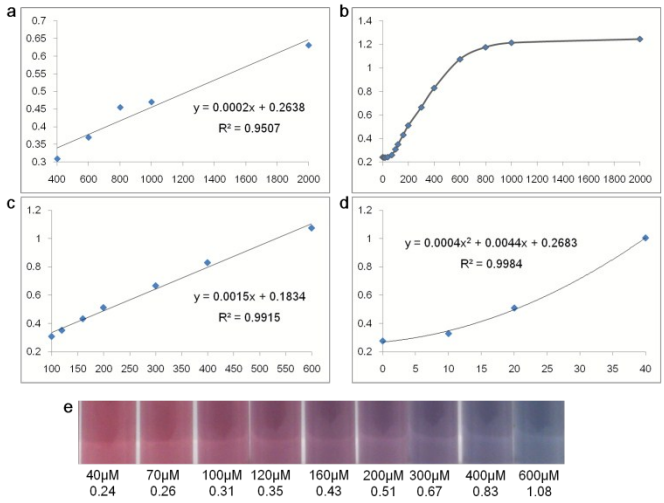

Fig. 3 Fitting of the absorption intensity ratio between 650 nm and 527 nm in AuNP solutions. Duration of incubation: a, 3 h 45 min; b and c, 6 h 31 min; d, 16 h 24 min. Unit of the abscissa is μM. e, Juxtaposition of sample color, H_2O_2 concentrations (μM), and intensity ratios obtained from the samples at 6 h 31 min.

Factors affecting the performance of this detection system may include temperature of incubation and ratio between the lipoic-phenylboronate-mPEG$_{5000}$ ligand and 1-hexanethiol on AuNP surface. Temperature of incubation influences the chemical reaction rate of the PEG ligand with H_2O_2 and the frequency of AuNP collision. Lower temperature would slow down the oxidation and hydrolysis of the PEG ligand in H_2O_2 solution and reduce the collision frequency of AuNPs. Hence, the color change rate of AuNPs should be slower. The experimental results (Fig. 4, 25 °C) well support this reasoning. Although the experiments exhibited a similar gradual progress of color change from high to low H_2O_2 concentrations, the time it took to clearly discriminate the color change for 10 μM sample was much longer (5-8 days, Fig. 4g,h), which is not suitable for practical use. Similarly, the rate of color change also followed a linear relationship (Fig. S4 in the ESI). In addition to the incubation temperature, the ratio of the two ligands on the AuNP surface is also a key element to affect the performance of this detection system. It is very difficult to accurately determine the ratio of two ligands on an AuNP surface, but this ratio should depend on the initial ratio of the two ligands added to the reaction solution. When increasing the amount of the lipoic-phenylboronate-mPEG$_{5000}$ ligand by 3 folds, the resulted AuNPs could not aggregate under the conditions where the original AuNPs could aggregate (Fig. S5 in the ESI). Though reducing the amount of the PEG ligand might in principle lead to faster response and lower limit of detection, it decreases the intrinsic stability of AuNPs and makes the color discrimination of blank AuNP sample and samples with lower concentrations of H_2O_2 unconvincing. Therefore, a balance between fast response/low detection limit and intrinsic stability of AuNPs should be taken into consideration.

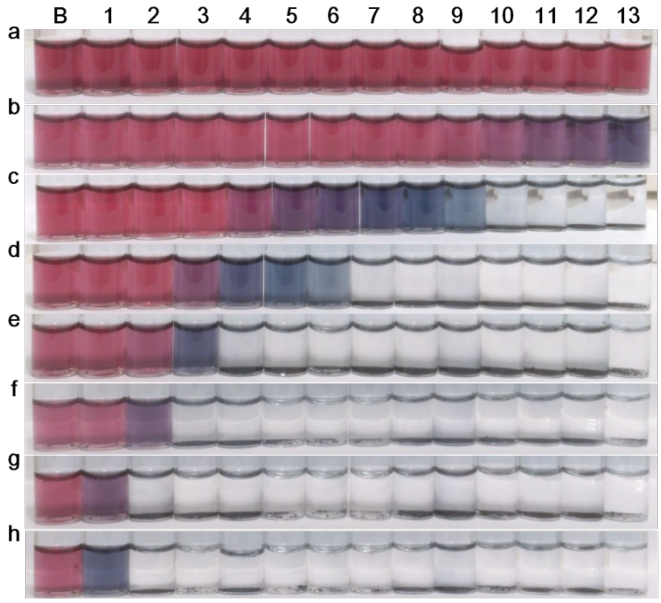

Fig. 4 Gradual aggregation and color change of AuNP solutions incubated with different concentrations of H_2O_2 at 25 °C. Column B: blank AuNP sample without H_2O_2. Columns 1-13: 10 μM, 20 μM, 40 μM, 70 μM, 100 μM, 120 μM, 160 μM, 200 μM, 300 μM, 400 μM, 600 μM, 800 μM, and 2 mM of H_2O_2. Duration of incubation: a, 0 h; b, 19 h; c, 34 h; d, 46 h; e, 62 h; f, 83 h; g, 140 h; h, 190 h.

In conclusion, we have designed an AuNP-based platform based on quinone methide rearrangement and hydrophilicity change of colloidal AuNPs for naked-eye detection of H_2O_2. The experimental results reveal a linear (or unitary quadratic) relationship between the AuNP aggregation rate and the concentration of H_2O_2 added over a wide range (10 to 2000 μM, Fig. 3), indicating that this approach could be used for quantitative detection of H_2O_2. The lowest concentration of H_2O_2 that could be discriminated by naked eye using the present system was 10 μM. In comparison, two recently reported AuNP-based systems[9,10] showed comparable detection limits (20 μM) but much narrower dynamic ranges (20-120 μM[9] and 10-100 μM[10]). Since H_2O_2 is a very important enzyme-related small molecule and these enzymes (i.e., GOx and HRP) are highly suitable to be used in ELISA[25], this AuNP-based detection system could be applied in ultrasensitive detection of disease-related biomarkers, where the concentration change of H_2O_2 that is numerically correlated to

the quantity of biomarker proteins in the ELISA technique is measured. In fact, it has been reported that ultrasensitive detection of biomarkers by naked eye could be realized if 20 μM of H_2O_2 is discriminated[9, 10] on account of high catalytic activity of the enzymes. The present system shows much wider dynamic range of detection and lower limit of detection, and up to 24 hours of detection should still lie in an acceptable time scale. The effect of incubation temperature and ligand ratio could be potentially tailored to optimize the performance of the system.

This research is supported by the National Research Foundation (NRF), Prime Minister's Office, Singapore under its Campus for Research Excellence and Technological Enterprise (CREATE) Programme–Singapore Peking University Research Centre for a Sustainable Low-Carbon Future, as well as the NTU-A*Star Silicon Technologies Centre of Excellence under program grant no. 11235100003.

Notes and references

1. C. Wong, K. Wong and X. Chen, *Appl. Microbiol. Biotechnol.*, 2008, **78**, 927-938.
2. P. Chelikani, I. Fita and P. C. Loewen, *Cell. Mol. Life Sci.*, 2004, **61**, 192-208.
3. P. Wentworth Jr., L. H. Jones, A. D. Wentworth, X. Zhu, N. A. Larsen, I. A. Wilson, X. Xu, W. A. Goddard III, K. D. Janda, A. Eschenmoser and R. A. Lerner, *Science*, 2001, **293**, 1806-1811.
4. X. Zhu, P. Wentworth, A. D. Wentworth, A. Eschenmoser, R. A. Lerner and I. A. Wilson, *Proc. Natl. Acad. Sci. U.S.A.*, 2004, **101**, 2247-2252.
5. E. A. Veal, A. M. Day and B. A. Morgan, *Mol. Cell*, **26**, 1-14.
6. T. J. Jonsson, L. C. Johnson and W. T. Lowther, *Nature*, 2008, **451**, 98-101.
7. D. R. Gough and T. G. Cotter, *Cell Death Dis.*, 2011, **2**, e213.
8. H. Jin, D. A. Heller, M. Kalbacova, J.-H. Kim, J. Zhang, A. A. Boghossian, N. Maheshri and M. S. Strano, *Nat. Nanotechnol.*, 2010, **5**, 302-309.
9. R. de la Rica and M. M. Stevens, *Nat. Nanotechnol.*, 2012, **7**, 821-824.
10. D. Liu, J. Yang, H.-F. Wang, Z. Wang, X. Huang, Z. Wang, G. Niu, A. R. H. Walker and X. Chen, *Anal. Chem.*, 2014, **86**, 5800-5806.
11. Z. Gao, M. Xu, L. Hou, G. Chen and D. Tang, *Anal. Chem.*, 2013, **85**, 6945-6952.
12. W. Lai, D. Tang, J. Zhuang, G. Chen and H. Yang, *Anal. Chem.*, 2014, **86**, 5061-5068.
13. L. Rodríguez-Lorenzo, R. de la Rica, R. A. Álvarez-Puebla, L. M. Liz-Marzán and M. M. Stevens, *Nat. Mater.*, 2012, **11**, 604-607.
14. J. L. Lyon and K. J. Stevenson, *Anal. Chem.*, 2006, **78**, 8518-8525.
15. M. E. Welch, N. L. Ritzert, H. Chen, N. L. Smith, M. E. Tague, Y. Xu, B. A. Baird, H. D. Abruña and C. K. Ober, *J. Am. Chem. Soc.*, 2014, **136**, 1879-1883.
16. A. Yu and F. Caruso, *Anal. Chem.*, 2003, **75**, 3031-3037.
17. P. D. Howes, R. Chandrawati and M. M. Stevens, *Science*, 2014, **346**.
18. J. Sun, Y. Xianyu and X. Jiang, *Chem. Soc. Rev.*, 2014, **43**, 6239-6253.
19. J. Wang, *Small*, 2005, **1**, 1036-1043.
20. Y. Zhang, Y. Guo, Y. Xianyu, W. Chen, Y. Zhao and X. Jiang, *Adv. Mater.*, 2013, **25**, 3802-3819.
21. W. Zhou, X. Gao, D. Liu and X. Chen, *Chem. Rev.*, 2015.
22. R. Liu, R. Liew, J. Zhou and B. Xing, *Angew. Chem., Int. Ed.*, 2007, **46**, 8799-8803.
23. D. Liu, Z. Wang, A. Jin, X. Huang, X. Sun, F. Wang, Q. Yan, S. Ge, N. Xia, G. Niu, G. Liu, A. R. H. Walker and X. Chen, *Angew. Chem., Int. Ed.*, 2013, **52**, 14065-14069.
24. A. J. Gormley, R. Chapman and M. M. Stevens, *Nano Lett.*, 2014, **14**, 6368-6373.
25. S. S. Deshpande, *Enzyme Immunoassays: From Concept to Product Development.* Chapman & Hall: New York, 1996.
26. S. Gnaim and D. Shabat, *Acc. Chem. Res.*, 2014, **47**, 2970-2984.
27. E. Sella, A. Lubelski, J. Klafter and D. Shabat, *J. Am. Chem. Soc.*, 2010, **132**, 3945-3952.
28. C. de Gracia Lux, S. Joshi-Barr, T. Nguyen, E. Mahmoud, E. Schopf, N. Fomina and A. Almutairi, *J. Am. Chem. Soc.*, 2012, **134**, 15758-15764.
29. R. Kumar, J. Han, H.-J. Lim, W. X. Ren, J.-Y. Lim, J.-H. Kim and J. S. Kim, *J. Am. Chem. Soc.*, 2014, **136**, 17836-17843.
30. T. Yoshii, S. Onogi, H. Shigemitsu and I. Hamachi, *J. Am. Chem. Soc.*, 2015, **137**, 3360-3365.

TOC Figure

Gold nanoparticle-based platform for naked-eye detection of H_2O_2 was realized by changing the surface hydrophilicity.